

Enhanced dewatering of waste-activated sludge by composite hydrolysis enzymes

Boran Wu¹ · Xiaoli Chai¹ · Youcai Zhao¹

Received: 4 October 2015 / Accepted: 8 January 2016 / Published online: 27 January 2016
© Springer-Verlag Berlin Heidelberg 2016

Abstract The feasibility of composite hydrolysis enzymes in enhanced dewatering of waste-activated sludge (WAS) was verified in this study. A Pearson correlation analysis was conducted to explore the roles of different extracellular polymeric substance (EPS) fractions on WAS dewaterability. The results indicated that tightly bound EPS (TB-EPS) was released into the liquid phase consistently during enzymatic hydrolysis to form soluble EPS (S-EPS) and loosely bound EPS and that the TB-EPS content was positively correlated with the capillary suction time of WAS. A kinetic analysis was carried out to gain further insights into the kinetic variation in TB-EPS removal. It was found that TB-EPS reduction fit a first-order kinetic model and that mild temperature (25–30 °C) and a slightly acidic condition were favorable for the improvement of enzyme activity. Solid phase extraction combined with UV–Vis spectroscopy analysis was used to characterize the processes of migration and transformation of the hydrophobic (HPO), transphilic and hydrophilic (HPI) fractions in EPS during the enzymatic process. The results revealed that HPO and HPI were mainly composed of PN and PS, respectively, and that the enzymatic hydrolysis could enhance the transformation of HPI from TB-EPS to S-EPS, which was the dominant mechanism of improving WAS dewaterability.

Keywords Waste-activated sludge · Enzyme · Dewatering · Kinetic model · Hydrophilic/hydrophobic

List of abbreviations

WAS	Waste-activated sludge
CST	Capillary suction time
EPS	Extracellular polymeric substances
S-EPS	Soluble EPS
LB-EPS	Loosely bound EPS
TB-EPS	Tightly bound EPS
PS	Polysaccharide
PN	Protein
SPE	Solid phase extraction
HPO	Hydrophobic
TPI	Transphilic
HPI	Hydrophilic
UV–Vis spectra	Ultraviolet–visible spectra
EEM	Three-dimensional excitation–emission matrix
PAM	Polyacrylamide
COD	Chemical oxygen demand

Introduction

Municipal wastewater treatment plants produce large amounts of waste-activated sludge (WAS) with a high water content (over 95 %). The huge quantities of WAS are the subject of great concern, because the sludge causes serious pollution problems when it is not appropriately treated and disposed [1]. The annual production of WAS in China is 6.25 million tons on a dry solids (DS) basis and more than 80 % of this amount is disposed by improper dumping without further dewatering or processing [2]. Conventional conditioners, polyacrylamide (PAM), polyferric chloride and lime, are still widely used in some pretreatment operations for thickening and dewatering; however, although the dosage is up to the

✉ Xiaoli Chai
xlchai@tongji.edu.cn

¹ State Key Laboratory of Pollution Control and Resource Reuse, Tongji University, 1239 Siping Road, Shanghai 200092, China

range of 50–100 mg/g dry solid (DS), they can achieve only 15–20 % water removal. In addition, the conventional conditioning methods limit the subsequent utilization of WAS and may lead to serious pollution risks, such as biological toxicity, increased likelihood of equipment corrosion and the potential to form dioxins during subsequent sludge incineration [3, 4]. In this regard, many physicochemical conditioning approaches, such as ultrasonication [5], microwave irradiation [6], freezing and thawing [7], and electro-dewatering [8], have also been developed. However, regardless of some dewatering potential of these methods, the large consumption of energy, the harsh operation conditions and the difficulty of application at engineering scale limited their popularization. Thus, it is urgent to develop efficient and environmentally friendly methods of WAS dewatering.

Extracellular polymeric substances (EPS) are formed by various biochemicals secreted by microbes, release of cellular material and products by cell lysis or organic matter in the medium [9]. EPS constitute a significant fraction of sludge mass and play a key role in binding a large volume of water (i.e., bound water) [10–12]. Especially, the negatively charged bound EPS network plays a significant role in maintaining a hydrated sludge structure and could effectively prevent the release of water [13]. Sludge hydrophobicity increases with the protein content of bound EPS, and an increased hydrophobic generally leads to a worse dewaterability [11]. Therefore, it is recognized that to a certain extent, the degradation of EPS and the lysis of sludge micro-organisms can enhance the release of water from sludge floc [14]. Accordingly, mixtures of hydrolysis enzymes, such as proteases, lipidases and carbohydrases, are gaining attention for use in improving WAS dewaterability by EPS hydrolysis [15–17]. The advantages of composite enzymes include non-toxicity, biodegradability and low dosage. The existing researches mainly focus on optimizing the process parameters of enzyme-assisted dewatering by batch experiments, for example Ayol et al. [15] and Lu et al. [17] confirmed the feasibility of dewatering sewage sludge and cellulosic sludge by hydrolysis enzyme, respectively, and Dental et al. [18] evaluated the performance of enzyme-assisted dewatering from the perspective of shear sensitivity of digested sludge. However, the enzymatic mechanism of action in the area of EPS composition variation has been hardly discussed in the literature.

In this study, the feasibility of composite hydrolysis enzymes on improving the dewaterability of WAS was verified in terms of the capillary suction time (CST). EPS composition changes and CST were monitored simultaneously to analyze the correlation between them. A kinetic model of EPS degradation was established to understand the effects of reaction conditions, temperature, pH and

enzyme dosage on enzymatic dewatering. Based on the separation of hydrophilic and hydrophobic components in EPS by solid phase extraction (SPE), UV–Vis and three-dimensional excitation–emission matrix (EEM) fluorescence techniques were used to explore the mechanism of enhancing sludge dewaterability from the perspective of changing hydrophilic and hydrophobic functional groups.

Methods and materials

Materials

The WAS used in this study was obtained from a wastewater treatment plant located in Shanghai, China, which has a design capacity of 150,000 m³/day. The collected sludge was stored at 4 °C before use. The main characteristics of the concentrated sludge were pH 6.96 ± 0.01, water content 99.32 ± 0.05 %, TS 6.82 ± 0.51 g/L, VSS 5.45 ± 0.49 g/L, CST 104.6 ± 6.2 s and specific resistance of filtration (SRF) 2.11 ± 0.12 × 10¹² cm/g.

The enzyme mixture, Enviro-zyme 216, was purchased from Winston Company, Tulsa, USA. It contains a complex enzyme mixture of protease and lipase and a kind of anaerobic bacteria, *Aspergillus oryza*. A fresh stock solution (2 %w/v) was prepared daily by adding the dry product to 37 °C water before conducting experiments. 37 °C was chosen as the preparation temperature of the stock solution according to the optimal temperature for the solubilization of extracellular enzyme secreted by *Aspergillus oryzae* [15]. All of the chemical reagents are of analytical grade unless otherwise stated.

Experimental procedure

The required amount of enzyme stock solution mentioned in 2.1 was added to WAS samples to give the desired enzyme concentration [15]. The sample was then subjected to moderate mixing (100 rpm using a magnetic stirrer) and incubated for 16 h at the predetermined temperature and pH. At different time intervals within 16 h, the 30 mL sludge samples were taken for dewaterability evaluation and EPS analysis. The sludge dewaterability was evaluated in terms of CST, using a standard CST apparatus (Type 304B, Triton Electronics Ltd., UK) with standard chromatography-grade CST paper. The chosen enzymes were secreted by the anaerobic fungus, *Aspergillus oryzae*. Hence, to harvest enzyme under normal conditions for *Aspergillus oryzae* metabolism, the serum bottles were purged with nitrogen gas and sealed with a rubber cap to maintain the anaerobic conditions used for the preparation of enzyme stock solution and incubation of sludge samples.

Procedure for EPS extraction and related analytical methods

Standard procedures for EPS extraction of sludge samples using centrifugation plus ultrasonication were modified based on a method detailed elsewhere [19]. In brief, the sludge was first centrifuged at $2000\times g$ for 15 min at 4 °C; the supernatant was soluble EPS (S-EPS). The sludge pellets were then resuspended and diluted to the original volume by adding 0.05 % NaCl solution. Afterward, the mixture was sheared by a vortex mixer (S25, IKA, Germany) for 2 min and then centrifuged at $5000\times g$ for 15 min at 4 °C. The organic matter in the collected supernatant was regarded as loosely bound EPS (LB-EPS). Finally, the WAS pellets left in the tube were again suspended to the original volume and treated by ultrasonication (40 kHz and 120 W for 2 min). The supernatant collected was tightly bound EPS (TB-EPS), while the sediment was left in the pellet.

The polysaccharide and protein levels of the EPS were measured by the anthrone method [20] with glucose as the standard and the Lowry–Folin method with BSA (bovine serum albumin) as the standard [21], respectively.

Separation of different EPS fractions by SPE

The separation method of different water-extractable EPS fraction by SPE was established based on the modification of a similar procedure to separate the hydrophilic/hydrophobic soluble substances in the effluent of wastewater treatment plants [22, 23], because these dissolved organic matters usually show similar compositions and properties of soluble EPS. A Poly-Sery HLB SPE (strong polarity)/neutral Al_2O_3 -XAD-2 SPE (non-polarity) (ANPEL, China) was used to fractionate EPS into hydrophobic (HPO), transphilic (TPI) and hydrophilic (HPI) fractions. A 3-mL sample of extracted EPS was first passed through the Poly-Sery HLB SPE, which was activated by successive treatments with 6 mL methanol and 6 mL deionized water. Then, the Poly-Sery HLB SPE was eluted with 6 mL methanol, and the HPO fraction was obtained. The remaining sample was passed through the neutral Al_2O_3 -XAD-2 SPE, which was activated by 25 mL 70 % ethanol and 25 mL deionized water. The HPI fraction was eluted from the neutral Al_2O_3 -XAD-2 SPE with 25 mL 70 % ethanol. The non-retained sample comprised the TPI fraction.

Ultraviolet visible (UV–Vis) spectra of the HPO, TPI and HPI fractions were recorded with a UV–visible spectrophotometer (UV-2550, Shimadzu Co., Japan) in a 1-cm quartz cuvette. The spectra were gathered with absorbance scanning from 200 to 700 nm at 1-nm increments and presented in terms of absorbance. Prior to collecting spectra of the EPS fractions, the UV–Vis spectra of the

solvents were collected under the same conditions to deduct the background signal.

Three-dimensional EEM fluorescence spectroscopy

EEM fluorescence spectra were obtained using a luminescence spectrometer (FluoroMax-4, HORIBA Jobin–Yvon Co., France). EEM spectra were collected with subsequent scanning emission spectra from 250 to 550 nm at 5-nm increments by varying the excitation wavelength from 250 to 400 nm at 5-nm increments. The excitation and emission slits were maintained at 10 nm and the scanning speed was set at 4800 nm/min for all of the measurements. A 290-nm emission cutoff filter was used during scanning to eliminate second-order Raleigh light scattering. Origin 9.0 software (Origin Lab Inc., USA) was used to handle the EEM data [24].

Statistical analysis

A statistical analysis was carried out using the software Origin 9.0 (Origin Lab Inc., USA). Pearson's correlation coefficient (R) was used to identify the strength of the linear correlation between two parameters. The correlation R can range between -1 and $+1$, where -1 , $+1$ and 0 denote a perfect negative correlation, a perfect positive correlation and the absence of a relationship, respectively. The correlations were considered statistically significant at a 95 % confidence interval ($p < 0.05$) [25].

Results and discussion

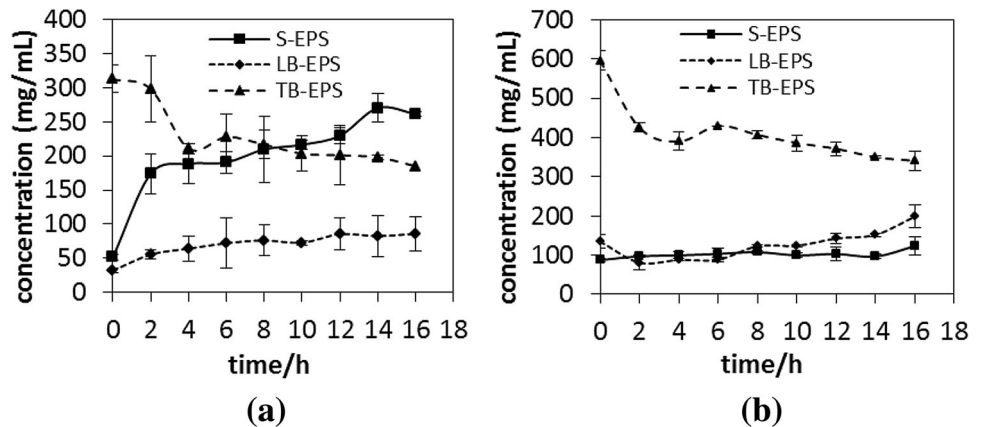
Effects of enzymatic pretreatment on WAS dewaterability

Variation of EPS components

In biological wastewater treatment systems, the chemical characteristics of EPS is diverse and varies in the concentrations and forms of their constituent carbohydrates (polysaccharide, PS), protein (PN), nucleic acid, lipids and humic substances (non-secreted fraction) [12, 26, 27]. It is expected that the enzymatic hydrolysis of the dominant macromolecule of EPS, proteins and carbohydrates (75–90 % of the total EPS mass) [28] will lead to the cleavage of WAS floc and be beneficial for the water removal from WAS, so the composition variation of different EPS fractions in the presence of enzyme was investigated first at the enzyme dosage of 1 mg/g DS and temperature of 30 °C.

As shown in Fig. 1a, the PN concentrations in raw sludge were estimated to be 51.84 ± 3.90 , 32.13 ± 3.25

Fig. 1 Composition variation of different EPS fractions: **a** PN, **b** PS



and 312.19 ± 20.14 mg/L of S-EPS, LB-EPS and TB-EPS for the untreated WAS, respectively. During enzymatic incubation, the PN concentration in TB-EPS decreased continuously from 312.19 ± 20.14 to 184.94 ± 3.25 mg/L; in contrast, it increased to 261.32 ± 3.90 and 86.10 ± 4.69 mg/L in S-EPS and LB-EPS, respectively. It was reported previously that not all floc structures are formed by orderly biochemical polymerization reactions, but there is a significant amount of macromolecular entrapment by non-specific interactions during the floc-forming process [29]. Therefore, the hydrolysis of TB-EPS with the enzymatic proceeding led to the cleavage of linkages among macromolecules in TB-EPS, such as peptide bonds ($-\text{CO}-\text{NH}-$) and hydrogen bonds and partially released PN into the liquid phase. The released PN was isolated as the S-EPS and LB-EPS fractions in this study, resulting in increasing contents of S-EPS and LB-EPS.

As shown in Fig. 1b, the concentration of PS in pretreated TB-EPS showed a decreasing trend similar to that for PN of TB-EPS, and the concentration of PS in LB-EPS also decreased from 95.36 ± 0.45 to 81.10 ± 0.19 mg/L in the first 2 h. The decrease in PS in bound EPS can be attributed to the hydrolysis of macromolecular compounds [29, 30]. However, as a result of the great reduction of TB-EPS, the PS concentration of LB-EPS kept growing consistently in the follow-up 14 h of incubation and PS in S-EPS also showed an obvious increase from 87.39 ± 3.88 to 123.33 ± 23.47 mg/L through the whole process, which was similar to the transformation of PN between bound EPS and S-EPS.

Variation of CST

CST was measured to evaluate the dewaterability of WAS pretreated by the composite enzymes. The batch test was also conducted at the enzyme dosage of 1 mg/g DS and temperature of 30 °C. As shown in Fig. 2, the CST decreased from 102.5 s to the lowest value, 53.5 s in the

first 8 h of incubation; then a slight deterioration of WAS dewaterability was observed from 8 to 10 h and CST stayed nearly constant from 10 to 16 h, which was consistent with previous reports [15, 16, 31]. It was reported that the combined addition of cellulase and protease resulted in an 80 % reduction in solids (20 % in the control), 93 % removal of particulate chemical oxygen demand (COD) (59 % in the control) and substantial increase of soluble COD after 16 h incubation [30]. An excessive solubilization of organic substances and breakdown of the polymeric matrix may increase the viscosity of WAS and weaken the dewatering performance [32]. Besides, due to the polymeric matrix breakdown, the release of supracolloidal particles resulted in a clogged filter medium, which limited the filtrate flow and increased the measured CST value [33].

Analysis of the correlation between dewaterability and EPS composition

The various components in EPS have different effects on the dewatering ability of microbial aggregates [12]. An increasing carbohydrate fraction in EPS would enhance the aggregation of sludge flocs according to previously reported results [34, 35]. On the contrary, the proteins had a high water-holding capacity due to the hydrogen bond induced by nitrogen-containing and oxygen-containing functional groups, entrapping water molecules in the gaps among chain-like macromolecules [34, 36]. The loosely packed sludge flocs consisting of hydrophobic proteins with a higher content of pore water and sticky matter would reduce the sludge compressibility and dewaterability [37]. But if the macromolecules are hydrolyzed into small fragments, the hydrophobic substances will dissolve into liquid phase and have little effect on the hydrophilicity of WAS. Thus, the Pearson analysis was conducted, so that the relationship between the dewaterability and different EPS fractions could be established. The results are shown

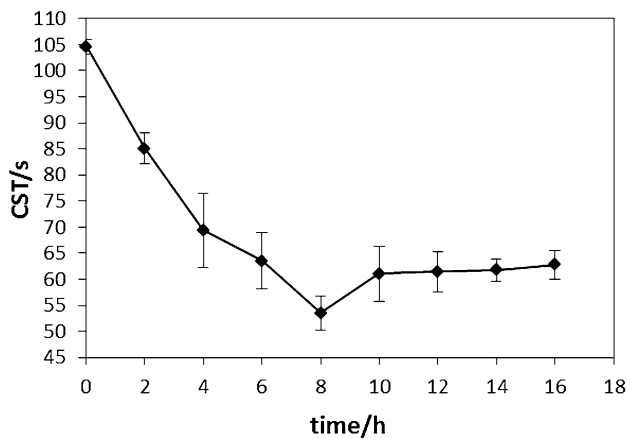


Fig. 2 CST variation of pretreated WAS

Table 1 Correlation between CST and EPS fraction: Pearson’s correlation coefficients (R_p) (p values in parenthesis)

	PN	PS	PN/PS	PN + PS
TB-EPS				
CST				
R_p	0.9159	0.8545	0.3106	0.9094
p value	5.231E-4	0.003350	0.4160	6.731E-4
LB-EPS				
CST				
R_p	-0.9320	-0.2264	-0.5001	-0.5188
p value	2.520E-4	0.5581	0.1704	0.1524
S-EPS				
CST				
R_p	-0.8766	-0.6263	-0.8339	-0.8789
p value	0.001920	0.07115	0.005210	0.001800

in Table 1. Values in bold refer to variables for which correlation is significant ($p < 0.05$).

The statistical analysis in Table 1 indicates that the CST correlated positively with the individual polymers PN, PS from TB-EPS and total TB-EPS (PN + PS). Also, CST correlated negatively with PN from S-EPS and LB-EPS, while no significant correlation was found between the dewaterability and PS, PN/PS from LB-EPS or PS from S-EPS. These results revealed that WAS dewaterability is strongly governed by PN in EPS rather than PS and is in good agreement with previous works [12]. The CST correlated negatively with PN/PS from S-EPS, which implied that the hydrolysis of protein and transamination of amino acids are beneficial for the removal of hydrophilic function groups (i.e., $-\text{NH}_2$) and improve WAS dewaterability [1]. Moreover, it is worth noting that PN located in different layers of the WAS floc structure could have positive or adverse effects on the dewaterability of WAS, which was also pointed out by Li et al. [37] and Sheng et al. [12]. This

Table 2 Correlation among different EPS fractions: Pearson’s correlation coefficients (R_p) (p values in parenthesis)

	PN in S-EPS	PN in LB-EPS
PN in TB-EPS		
R_p	-0.8673	-0.9132
p value	5.8100E-04	0.002460
PS in S-EPS		
PS in LB-EPS		
PS in TB-EPS		
R_p	-0.6517	-0.8865
p value	0.05720	0.003350

If the p value is lower than 0.05, the corresponding R_p is significant. The significant data are in bold

phenomenon may depend on the PN chemical structure change induced by the added enzyme. Therefore, investigating the migration and transformation of hydrophilic and hydrophobic components in different EPS fractions in the following sections will be valuable for further understanding the mechanism of enzymatic WAS dewatering.

Pearson correlation among different EPS fractions is shown in Table 2. It can be found that PN from S-EPS and LB-EPS both oppositely correlated with PN from TB-EPS ($R_p = -0.8673$, $p < 0.05$; $R_p = -0.9132$, $p < 0.05$). PS from TB-EPS and LB-EPS also showed a close correlation ($R_p = -0.8865$, $p < 0.05$). These results partly verified the hypothesis that when the WAS flocs was disrupted with hydrolysis, a part of TB-EPS were solubilized and released into the liquid phase, thereby increasing the S-EPS and LB-EPS levels.

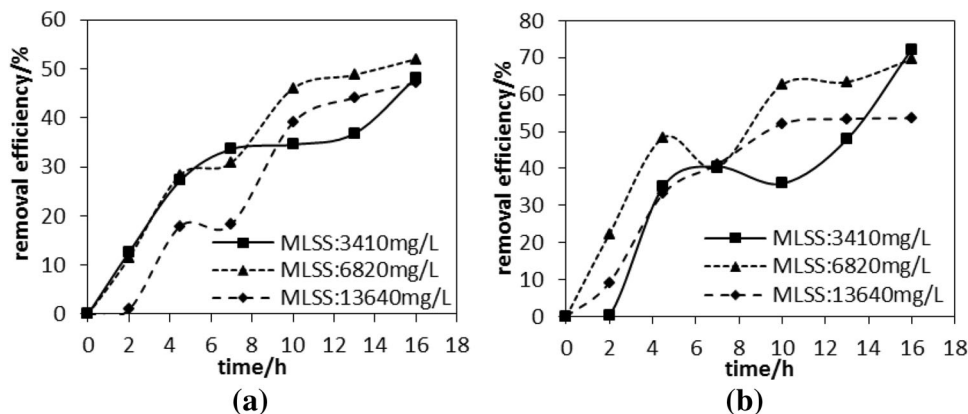
Kinetic study of the enzymatic reaction

According to the results from “Effects of enzymatic pretreatment on WAS dewaterability” section, the CST reduction of WAS was closely correlated with the removal of TB-EPS, and the increase of S-EPS and LB-EPS was also partially attributed to the TB-EPS degradation. Therefore, TB-EPS plays a key role in the enzymatic improvement of WAS dewaterability. A kinetic analysis was carried out to gain further insights into the kinetic variation of TB-EPS reduction and lay a theoretical foundation for optimizing the enzymatic reaction conditions (temperature, pH and enzyme dosage) from the perspective of the reaction kinetics.

Preliminary study of the enzymatic degradation of EPS

It is well known that the kinetics of enzymatic reactions can be described by the Michaelis–Menten equation, $V = V_{\max} \times [S]/([S] + K_m)$, where V is the reaction rate, $[S]$ is the substrate concentration and K_m is the half-

Fig. 3 Removal efficiency of TB-EPS: **a** PN, **b** PS



saturation constant. K_m and V_{max} are determined by the characteristics of the enzyme. Thus, applying an appropriate ratio of enzyme and substrate concentration is very important to improve the enzymatic reaction efficiency. In this study, the dosage of composite enzymes was controlled at a fixed value, and then the effect of initial EPS concentration on PN and PS removal efficiency was investigated by kinetic analysis. The kinetic analysis can be used to evaluate the applicability of enzymes for the hydrolysis of substrates in WAS and lays a theoretical foundation for improving the enzymatic reaction efficiency.

Three identical reactors were charged with initial MLSS of WAS of 3410, 6820 and 13,640 mg/L (by diluting or concentrating the WAS as described in “Materials”) and were maintained at 30 °C. The dosage of enzyme was kept at 1 mg/g DS. During the enzymatic reaction, the trends of the removal efficiency of PN and PS from TB-EPS with treatment time at different MLSS are illustrated in Fig. 3a, b, respectively. It can be found that at some specific time intervals within 16 h, reactors with different initial concentrations of TB-EPS attained similar removal efficiency. It seems that the removal efficiency was ultimately independent of the initial concentration of TB-EPS during the 16 h of incubation. According to recognized reports, the relation between the initial concentration of reactant and its conversion efficiency within the same reaction time and steady environmental conditions (temperature and pH) was as follows: negatively correlated during zero-order reaction, not correlated during first-order reaction and positively correlated during second-order reaction [38]. Thus, it can be inferred that the enzymatic reaction matches the first-order kinetics. In addition, according to the Michaelis–Menten equation, only when $[S]$ is far lower than K_m can the enzymatic reaction be approximated as a first-order reaction. Therefore, it can be determined that the introduced enzyme concentration of 1 mg/g is adequate for the degradation of the corresponding substrate in WAS. Excessive enzyme is meaningless for the improvement of WAS dewaterability, and the environmental factors

(temperature and pH) should be attached importance to the optimization of WAS enzymatic dewatering.

Effect of temperature on the kinetic constant

The composite enzyme used in the study is secreted from *Aspergillus oryzae*; thus, the reaction temperature is chosen based on the preferential temperature (25–35 °C) of the culture of *Aspergillus oryzae* and megatemperature should be avoided to limit its negative effect on enzyme activity. Based on the discussion in “Preliminary study of the enzymatic degradation of EPS”, the enzymatic removal of TB-EPS can be described by the following first-order kinetic equation:

$$V = -\frac{dX}{dt} = k_e \times X \quad (1)$$

$$\ln X = -k_e \times t + b, \quad (2)$$

where V is the reaction rate, X is PN or PS of TB-EPS, k_e (h^{-1}) the enzymatic rate constant and b the constant of integration. The effect of temperature on the rate constant was investigated under the condition as follows: the dosage of the enzyme was 1 mg/g DS and pH was kept at the initial value. By plotting $\ln X$ versus t , the slope and the intercept can be obtained, which correspond, respectively, to the value of k_e and b in Eq. (1).

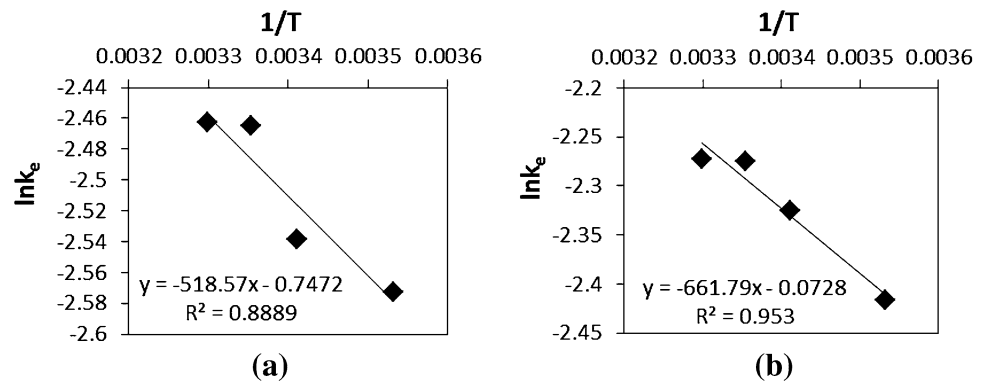
The values of k_e and b from 10 to 30 °C are shown in Table 3. It is clear that the R -squared values at different temperatures were reassuringly in the range of 0.91–0.97, which is much higher than the R -squared value obtained from fitting the equations based on zero-order or second-order reactions (these data are not shown). This further demonstrated that the enzymatic release of TB-EPS in WAS obeyed first-order kinetics. Moreover, the rate constants k_e of PN and PS reduction both increased as temperature increased from 10 to 30 °C, while similar kinetic constants were obtained at 25 and 30 °C.

The Arrhenius equation attempts to establish the relationship between the rate constant and the reaction temperature.

Table 3 Kinetic constants at different temperatures

Temperature (°C)	Protein			Polysaccharide		
	K_e	B	R^2	k_e	b	R^2
10	0.07630	6.139	0.9687	0.0892	5.398	0.9158
20	0.07900	6.228	0.9553	0.0978	5.471	0.9544
25	0.08500	6.326	0.9631	0.1028	5.462	0.9241
30	0.08520	6.297	0.9538	0.1031	5.404	0.9513

Fig. 4 $\ln k_e$ as a function of $1/T$. **a** PN in TB-EPS, **b** PS in TB-EPS



$$k_e = A \times \exp\left(-\frac{E_a}{RT}\right), \tag{3}$$

where A is the pre-exponential factor, E_a (kJ/mol) the activation energy of the reaction and T (K) the absolute temperature. When the enzymatic removal of TB-EPS in WAS proceeds at the initial pH and temperature in the range of 10–30 °C, the relationship between $\ln k_e$ and $1/T$ is shown in Fig. 4. Obviously, the first-order hydrolysis rate constants obtained in this study followed an Arrhenius type of behavior; the activation energies E_a for PN and PS hydrolysis were 4.311 and 5.502 kJ/mol, respectively. Thus, the value of the first-order hydrolysis constant in the temperature range of 10–30 °C, k_e can be expressed by Eqs. (4) and (5):

$$k_e \text{ (PN)} = 0.4737 \times \exp\left(-\frac{4.311 \times 10^3}{RT}\right), \tag{4}$$

$$k_e \text{ (PS)} = 0.9298 \times \exp\left(-\frac{5.502 \times 10^3}{RT}\right). \tag{5}$$

From Table 3, it can be seen that the value of b remained almost constant in the temperature range of 10–30 °C. The average values of b for PN and PS hydrolysis are 6.247 and 5.434, respectively. Accordingly, the kinetic models of PN and PS in TB-EPS can be simplified as follows (t is reaction time):

$$X(\text{PN in TB-EPS}) = 516.46 \exp(-0.4737) \times \exp\left(-\frac{4.311 \times 10^3}{RT}\right) \times t \tag{6}$$

$$X(\text{PS in TB-EPS}) = 229.06 \exp(-0.9298) \times \exp\left(-\frac{5.502 \times 10^3}{RT}\right) \times t \tag{7}$$

Effect of pH on the kinetic constant

The values of k_e and b at different pH values are shown in Table 4. The reaction conditions were controlled as follows: temperature 30 °C and enzyme dosage 1 mg/g DS.

From Table 4, it can be seen that the highest rate constant of protease was 0.1035 at pH 6. Compared with the results collected from the experiment at the initial pH of WAS (Table 3), the slightly acidic condition was quite beneficial for improving protease activity. In contrast, the rate constant of PS solubilization from TB-EPS to the liquid phase decreased with increasing pH. The pH can vary the rate constant by influencing the chemical structure (i.e., ionization state) of enzymes, which can limit the specific interaction between the enzymes and substrates [39, 40]. Moreover, an alkaline pH may increase the zeta

Table 4 Kinetic constants at different pH values

pH	Protein			Polysaccharide		
	k_e	b	R^2	k_e	b	R^2
3	0.08760	6.304	0.9661	0.1146	6.652	0.9620
6	0.1035	6.814	0.9768	0.1045	6.623	0.9584
9	0.08970	6.955	0.9619	0.09210	6.523	0.9540
11	0.08730	6.884	0.9745	0.08990	6.556	0.9672

potential of WAS and result in electrostatic repulsion among solid particles, which inhibits the adsorption or diffusion of carbohydrate enzyme to polysaccharides in the interior of the sludge floc [41]. As a result, the rate constant of the enzymatic reaction decreased as the pH increased from 6 to 11.

Mechanism of enzymatic WAS dewatering

Migration and transformation of hydrophilic and hydrophobic components in different EPS fractions

UV–vis spectroscopy has been reported to be a sensitive method of identifying the representative functional groups of different EPS fractions. There are two main absorbance bands at approximately 210–240 and 250–280 nm in the representative UV–Vis spectra of EPS extracted from WAS. The absorbance band in the range from 210 to 240 nm can be linked to the presence of carboxylic bonds (–COOH) [42]. The latter absorbance band (wavelength range of 250–280 nm) present may represent C=O bonds and C=C bonds (or chromophores) [43, 44]. A scientific attempt was made to characterize the hydrophilic and hydrophobic components of EPS separated by SPE in this study. The reaction conditions were controlled as follows:

temperature 30 °C, enzyme dosage 1 mg/g DS and initial pH 6.

Definitely, changes in the UV–Vis spectra before and after pretreatment are reflections of the migration and transformation of the hydrophilic and hydrophobic components. The adsorption at approximately 250 nm of the pretreated TB-EPS fraction decreased compared with the TB-EPS isolated from raw sludge, which can be found in Fig. 5a. On the contrary, the 255–279 nm absorbance band of S-EPS isolated from pretreated WAS (Fig. 5c) was much wider than that from raw WAS. These two changes of UV–Vis spectra revealed that PN constituted the majority of the hydrophilic components in EPS, because the 255–279-nm absorbance band refers to the representative functional group, C=O, of PN [42, 45]. The proteins had a high water-holding capacity [34, 36], whereas PN released into S-EPS, which is evenly distributed in the liquid phase, is more easily removed together with free water during the filtration process [25]. Therefore, the hydrolysis enzyme promoted the release of hydrophilic components (PN) from TB-EPS into S-EPS and resulted in the improvement of WAS dewaterability. LB-EPS is believed to produce highly porous sludge flocs with a lower density and a high amount of bound water [37]. However, according to Fig. 5b, no obvious increase

Fig. 5 UV–Vis absorbance spectra of HPI in different EPS fractions: **a** TB-EPS, **b** LB-EPS, **c** S-EPS

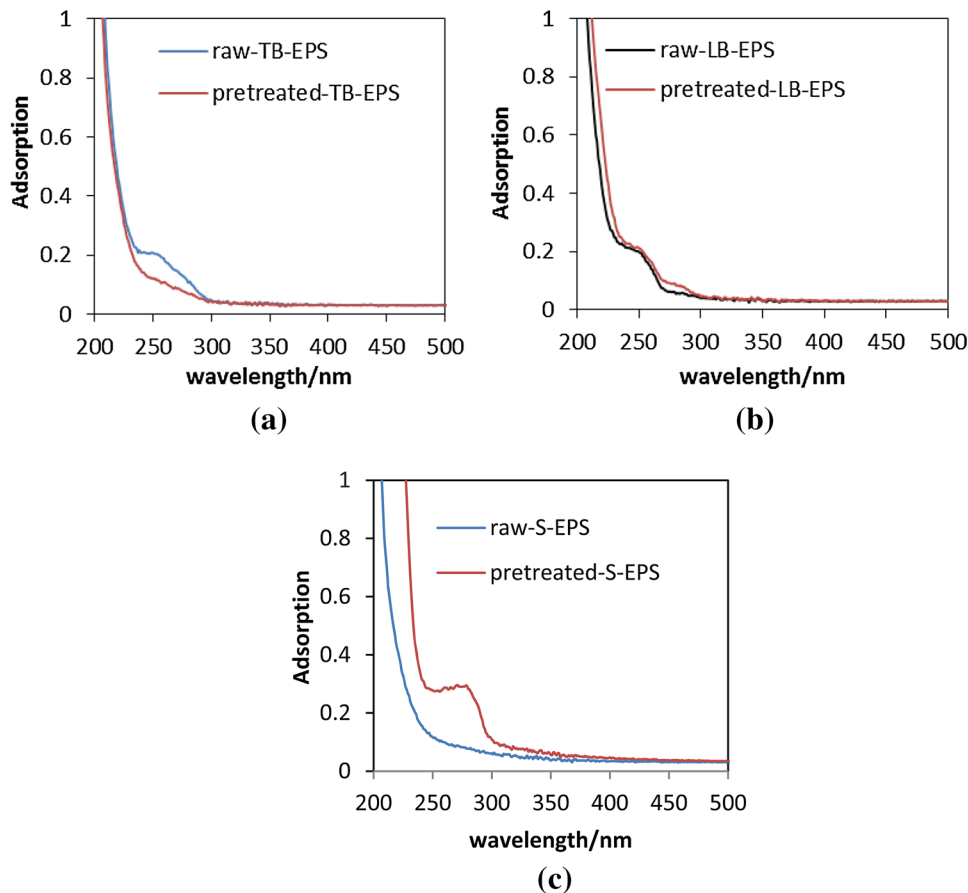


Fig. 6 UV–Vis absorbance spectra of HPO in different EPS fractions: **a** TB-EPS, **b** LB-EPS, **c** S-EPS

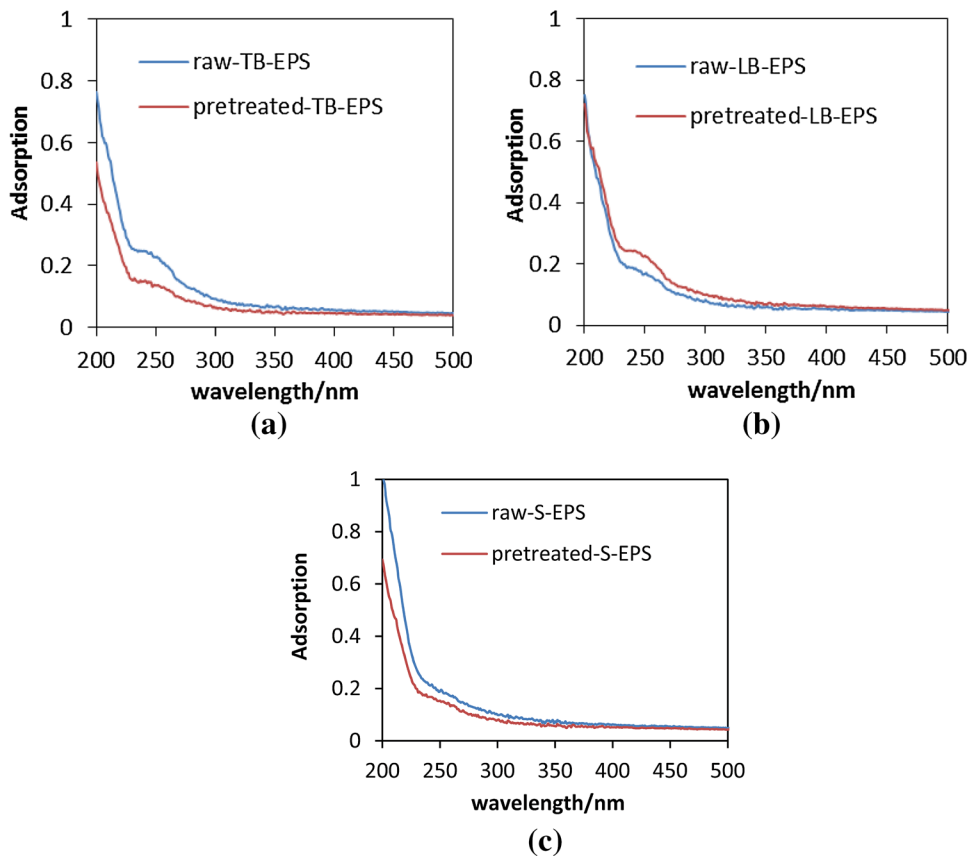
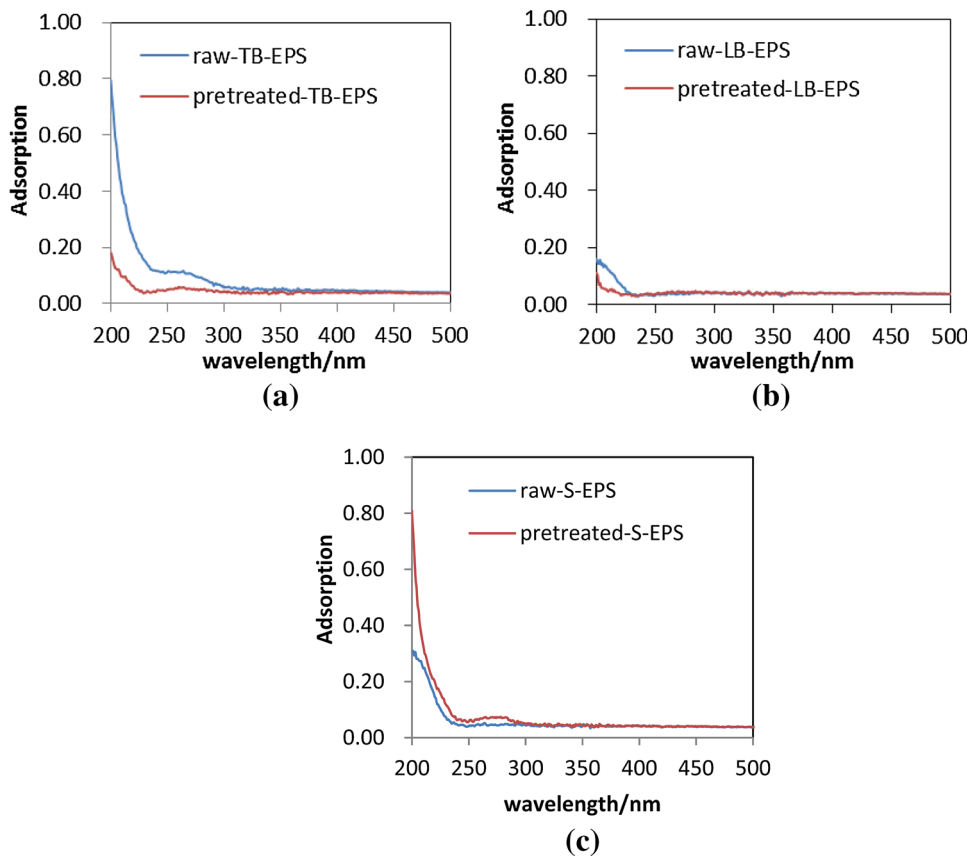


Fig. 7 UV–Vis absorbance spectra of TPI in different EPS fractions: **a** TB-EPS, **b** LB-EPS, **c** S-EPS



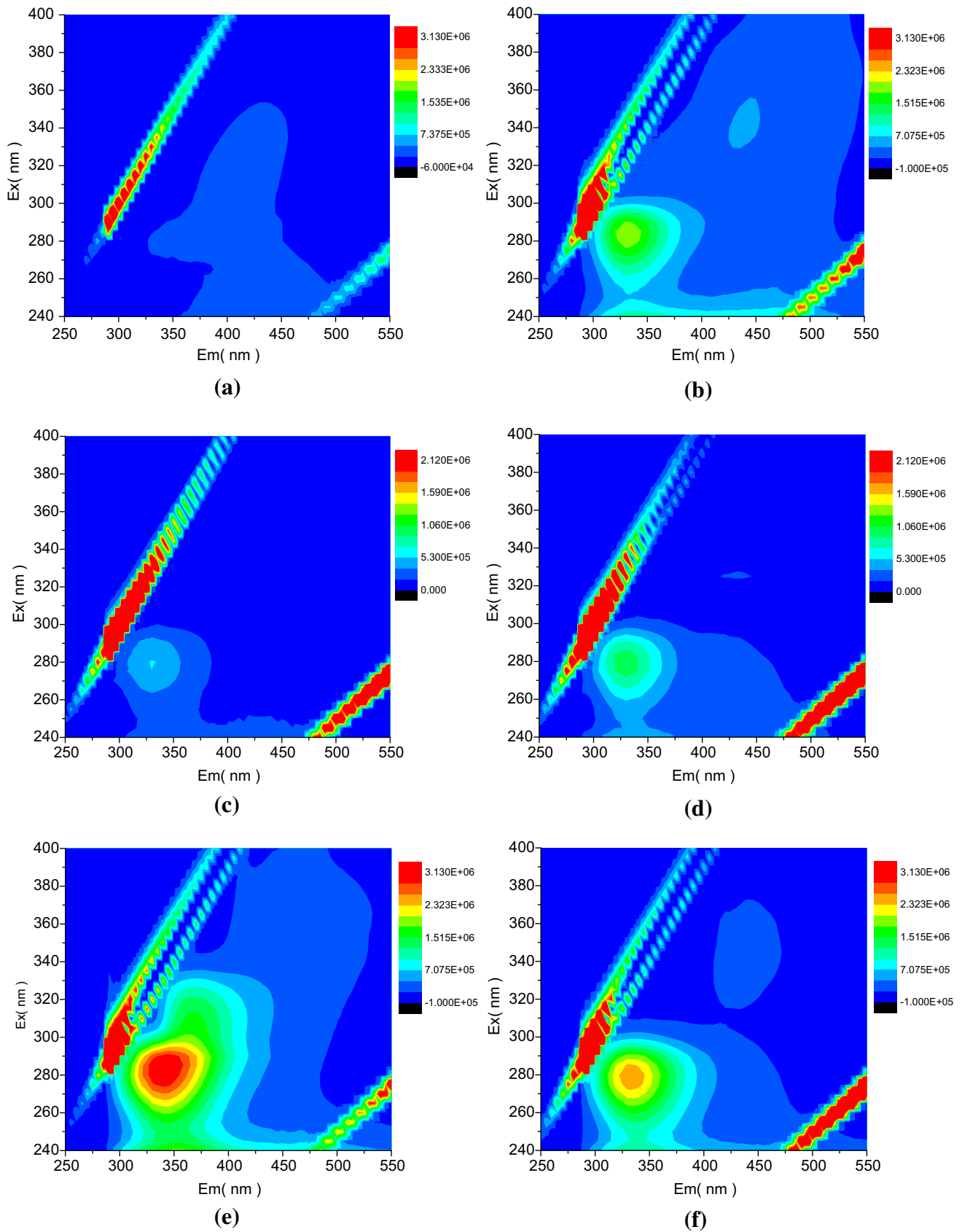


Fig. 8 EEM spectra of different EPS fractions: **a** S-EPS of raw WAS, **b** S-EPS of pretreated WAS, **c** LB-EPS of raw WAS, **d** LB-EPS of pretreated WAS, **e** TB-EPS of raw WAS, **f** TB-EPS of pretreated WAS

in HPI was found in LB-EPS after the enzymatic treatment.

Compared with the UV–Vis spectra of HPI, the absorbance bands of HPO were mainly located at wavelengths smaller than 250 nm, which demonstrated the effectiveness of hydrophilic/hydrophobic separation by SPE and confirmed the existence of carboxyl groups in HPO. Extracellular polysaccharides are composed of dextran, cellulose, alginate, xanthan, gellan and hyaluronic acid [28]. Carboxyl groups are among the characteristic functional groups of some polysaccharides (alginate, xanthan, gellan and hyaluronic acid) [28], so the absorbance band at wavelengths of 220–250 nm can be regarded as the signal of polysaccharides and humic-like or fulvic-like substances with carboxylic acids and methoxy carbonyls. From Fig. 6a, it can be seen that the absorbance of pretreated TB-EPS is lower than that of raw TB-EPS, which was consistent with the reduction of TB-EPS induced by enzymatic hydrolysis. In the case of LB-EPS, the absorbance band of pretreated WAS had higher relative intensities than that of raw WAS, which indicated the transformation of carbohydrate into LB-EPS during enzymatic hydrolysis (Fig. 6b). The increasing carbohydrate fraction in LB-EPS is closely correlated with the improvement of compressibility and enhanced sludge dewatering [34, 35].

Broad absorbance bands with low intensity were obtained in the UV–Vis spectra of TPI (Fig. 7). The featureless UV–Vis spectra reflected the complexity of TPI composition, and the low relative intensity, especially for LB-EPS, indicated the small proportion of TPI in total EPS. A lower absorbance of pretreated TB-EPS compared to that of raw TB-EPS was observed in the spectra of TPI, which again highlights the decomposition and release of TB-EPS. In addition, a slight absorbance band from 257 to 285 nm appeared in the UV–Vis spectra of S-EPS from pretreated WAS, and the pretreated S-EPS exhibited a higher absorbance at 200 nm. These can be linked to the transformation of C=O and C=C from cell lysis and intercellular substances into the liquid phase. Generally, the enzymatic reaction resulted in the destruction of bound EPS and was considerably favorable for the enhancement of WAS dewaterability.

EEM spectra of different EPS fractions

Three-dimensional EEM fluorescence spectroscopy, a rapid, selective and sensitive technique, can be regarded as

an overall “fingerprint” of samples that cover key components in cell metabolism, such as vitamins, NADH and amino acids (e.g., tryptophan) [46, 47]. Thus, EEM fluorescence spectroscopy may be appropriate for distinguishing the variation of fluorescence compounds present in EPS.

No obvious peak could be identified from the fluorescence spectra of raw S-EPS (Fig. 8a), whereas for the spectra of pretreated S-EPS (Fig. 8b), the peak intensity at excitation/emission wavelengths (Ex/Em) of 285 nm/330–348 nm increased significantly. The fluorescence peak was attributed to protein-like substances containing tryptophan, tyrosine and protein-like compounds [48]. In addition, the increasing protein-like fluorescence intensity is in good agreement with the increasing trend of protein content in S-EPS (Figs. 1a, 3a) and the increasing UV₂₅₀ absorbance of HPI in S-EPS during enzymatic pretreatment (Fig. 5c). In the case of LB-EPS from raw WAS and pretreated WAS (Fig. 8c, d), the main fluorescence peaks were both located at the Ex/Em of 270–280/330 nm due to the tryptophan protein present, but the difference in the fluorescence intensity verified the release of PN into LB-EPS from the inner layers of WAS flocs. For TB-EPS from pretreated sludge, the location of the fluorescence peak related to tryptophan-like protein showed a slight blue shift in terms of the emission wavelength compared with raw TB-EPS (raw TB-EPS: Ex/Em of 280/345–350 nm, pretreated TB-EPS: Ex/Em of 280/330 nm), which implied the elimination of particular hydrophilic groups, such as carbonyl, hydroxyl and amine, and a reduction in the number of aromatic rings and conjugated bonds in the chain structure [49–51]. The reduction can also be inferred from the decreasing UV₂₅₀ absorption of HPI in TB-EPS (Fig. 5a). Thus, the enzyme not only accelerated the removal of TB-EPS by hydrolysis, but also induced the directional transformation of some hydrophilic groups. According to previous reports, the hydrophilic components, protein-like substances in EPS, contributed more to the filtration resistance of membranes in MBRs [50, 51], so the decrease in hydrophilic groups in EPS was inevitably related to the enhanced dewaterability of WAS.

Conclusions

Composite hydrolysis enzymes were verified to be effective in enhanced dewatering of WAS, with a reduction in CST by 48.8 % at an extremely low enzyme dosage of 1 mg/g DS. The content of S-EPS and LB-EPS in WAS increased after the pretreatment with the composite enzymes, but the TB-EPS content decreased greatly during the enzymatic reaction. Pearson correlation analysis revealed that the TB-EPS content was closely positively correlated with the CST

of WAS and the increasing S-EPS and LB-EPS levels were also partially attributed to the TB-EPS removal. A kinetic model of TB-EPS removal was established; it was confirmed that TB-EPS reduction obeyed a first-order kinetic model. The rate constant for PN and PS reduction increased from 0.0763 to 0.0852 and 0.0892 to 0.1031 h⁻¹, respectively, as the temperature increased from 10 to 30 °C. A weakly acidic condition (pH 6–7) is beneficial for improving the rate constant of PN reduction, but the rate constant for PS reduction decreased consistently with increasing pH from 3 to 11. The optimal pretreatment conditions can be summarized as follows: 1 mg/g dry solid (DS) composite hydrolysis enzymes, temperature 30 °C and initial pH 6.0. The SPE combined with UV–Vis spectroscopy analysis found that HPI and HPO in EPS were mainly composed of PN and PS, respectively, and that enzymatic hydrolysis could enhance the transformation of HPI from TB-EPS to S-EPS, which resulted in the breakage of the WAS microfloc structure and was the dominant mechanism of improving WAS dewaterability.

Acknowledgments The authors wish to thank the Major Science and Technology Program for Water Pollution Control and Treatment (2013ZX07315-002) for their financial support of this study.

References

- Mowla D, Tran HN, Allen DG (2013) A review of the properties of biosludge and its relevance to enhanced dewatering processes. *Biomass Bioenergy* 58(21):365–378
- Yang G, Zhang G, Wang H (2015) Current state of sludge production, management, treatment and disposal in China. *Water Res* 78:60–73
- Magdalena KM, Renata ZT, Sabina B, Grzegorz B (2011) Yeast *Saccharomyces cerevisiae* devoid of Cu, Zn-superoxide dismutase as a cellular model to study acrylamide toxicity. *Toxicol In Vitro* 25(2):573–579
- Krause HH (1986) High temperature corrosion problems in waste incineration systems. *J Mater Energy Syst* 7(7):322–332
- Feng X, Deng J, Lei H, Bai T, Fan Q, Li Z (2009) Dewaterability of waste activated sludge with ultrasound conditioning. *Bioresour Technol* 100(3):1074–1081
- Yu Q, Lei H, Yu G, Feng X, Li Z, Wu Z (2009) Influence of microwave irradiation on sludge dewaterability. *Chem Eng J* 155:88–93
- Diak J, Ormeci B, Proux C (2011) Freeze-thaw treatment of RBC sludge from a remote mining exploration facility in subarctic Canada. *Water Sci Technol* 63(6):1309–1313
- Akrama M, Jérémy O, Jean V, Hoadley AFA (2010) Electrical field: a historical review of its application and contributions in wastewater sludge dewatering. *Water Res* 44(8):2381–2407
- Flemming HC, Wingender J (2001) Relevance of microbial extracellular polymeric substances (EPSs)—Part I: structural and ecological aspects. *Water Sci Technol* 43(6):1–8
- Mikkelsen LH, Keiding K (2002) Physico-chemical characteristics of full scale sewage sludges with implications to dewatering. *Water Res* 36(10):2451–2462
- Liu Y, Fang Herbert HP (2003) Influences of extracellular polymeric substances (EPS) on flocculation, settling, and dewatering of activated sludge. *Crit Rev Environ Sci Technol* 33(3):237–273
- Sheng GP, Yu HQ, Li XY (2010) Extracellular polymeric substances (EPS) of microbial aggregates in biological wastewater treatment systems: a review. *Biotechnol Adv* 28(6):882–894
- He DQ, Wang LF, Jiang H, Yu HQ (2015) A Fenton-like process for the enhanced activated sludge dewatering. *Chem Eng J* 272:128–134
- Neyens E, Baeyens J, Dewil R, Heyder BD (2004) Advanced sludge treatment affects extracellular polymeric substances to improve activated sludge dewatering. *J Hazard Mater* 106(2–3):83–92
- Ayol A (2005) Enzymatic treatment effects on dewaterability of anaerobically digested biosolids-I: performance evaluations. *Process Biochem* 40(7):2427–2434
- Ayol A, Dentel SK (2005) Enzymatic treatment effects on dewaterability of anaerobically digested biosolids-II: laboratory characterizations of drainability and filterability. *Process Biochem* 40(7):2435–2442
- Lu J, Rao S, Le T, Mora S, Banerjee S (2011) Increasing cake solids of cellulosic sludge through enzyme-assisted dewatering. *Process Biochem* 46(1):353–357
- Dentel SK, Dursun D (2009) Shear sensitivity of digested sludge: comparison of methods and application in conditioning and dewatering. *Water Res* 43(18):4617–4625
- Yu G, He P, Shao L, Lee D (2007) Enzyme activities in activated sludge flocs. *Appl Microbiol Biotechnol* 77(3):605–612
- Gaudy AF (1962) Colorimetric determination of protein and carbohydrate. *Ind Water Wastes* 7(1):17–22
- Lowry OH, Rosebrough NJ, Farr AL, Randall RJ (1951) Protein measurement with the folin phenol reagent. *J Biol Chem* 193(1):265–275
- Chai X, Liu G, Xin Z, Hao Y, Zhao Y (2012) Complexion between mercury and humic substances from different landfill stabilization processes and its implication for the environment. *J Hazard Mater* 209–210(1):59–66
- Malcolm RL, Maccarthy P (1992) Quantitative evaluation of XAD-8 and XAD-4 resins used in tandem for removing organic solutes from water. *Environ Int* 18(6):597–607
- Zhen G, Lu X, Zhao Y, Chai X, Niu D (2012) Enhanced dewaterability of sewage sludge in the presence of Fe(II)-activated persulfate oxidation. *Bioresour Technol* 116:259–265. doi:10.1016/j.biortech.2012.01.170
- Zhen GY, Lu XQ, Li YY, Zhao YC (2013) Innovative combination of electrolysis and Fe(II)-activated persulfate oxidation for improving the dewaterability of waste activated sludge. *Bioresour Technol* 136(3):654–663
- Massimiliano M, Pieter TV, Lilliam CM (2010) Exopolymeric substances (EPS) from *Bacillus subtilis*: polymers and genes encoding their synthesis. *FEMS Microbiol Lett* 313(1):1–9
- Simões M, Simões LC, Vieira MJ (2010) A review of current and emergent biofilm control strategies. *Lebensmittel-Wissenschaft und-Technologie* 43(4):573–583
- More TT, Yadav JSS, Yan S, Tyagi RD, Surampalli RY (2014) Extracellular polymeric substances of bacteria and their potential environmental applications. *J Environ Manage* 144(21):1–25
- Sesay ML, Özcengiz G, Sanin FD (2006) Enzymatic extraction of activated sludge extracellular polymers and implications on bioflocculation. *Water Res* 40(7):1359–1366
- Burgess JE, Roman BIPHJ (2009) Enzyme treatment to decrease solids and improve digestion of primary sewage sludge. *Afr J Biotechnol* 5(10):963–967
- Thomas L, Jungschaffer G (1993) Improved sludge dewatering by enzymatic treatment. *Water Technol* 28(1):189–192
- Gharibi H, Sowlat MH, Mahvi AH, Keshavarz M, Safari MH, Lotfi S, Abadi MB, Alijanzadeh A (2013) Performance

- evaluation of a bipolar electrolysis/electrocoagulation (EL/EC) reactor to enhance the sludge dewaterability. *Chemosphere* 90(4):1487–1494
33. Raynaud M, Vaxelaire J, Olivier J, Dieudé-Fauvel E, Baudez JC (2012) Compression dewatering of municipal activated sludge: effects of salt and pH. *Water Res* 46(14):4448–4456
 34. Cetin S, Erdinçler A (2004) The role of carbohydrate and protein parts of extracellular polymeric substances on the dewaterability of biological sludges. *Water Sci Technol* 50(9):49–56
 35. Jin B, WilWilén B-M, Lant P (2004) Impacts of morphological, physical and chemical properties of sludge flocs on dewaterability of activated sludge. *Chem Eng J* 98(1):115–126
 36. Sponza DT (2002) Extracellular polymer substances and physicochemical properties of flocs in steady and unsteady-state activated sludge systems. *Process Biochem* 37(9):983–998
 37. Li XY, Yang SF (2007) Influence of loosely bound extracellular polymeric substances (EPS) on the flocculation, sedimentation and dewaterability of activated sludge. *Water Res* 41(5):1022–1030
 38. Hill G, Charles, Root TW (2014) Basic and applied aspects of biochemical transformations and bioreactors. Wiley, Hoboken
 39. Chen Y, Liu K, Su Y, Xiong Z, Qin W (2013) Continuous bio-production of short-chain fatty acids from sludge enhanced by the combined use of surfactant and alkaline pH. *Bioresour Technol* 140(3):97–102
 40. Zhang C, Chen Y, Liu Y (2008) Effect of pH on enzyme activity involved in enhanced biological phosphorus removal system. In: *Proceedings of 13th international biotechnology symposium and exhibition*, vol 136, supplement issue, pp S647–S677
 41. Wingender J, Neu TR, Flemming H-C (1999) Extracellular polymeric substances. Characterization, structure and function. *Currentence* 88(1):45–53
 42. Vergnoux A, Rocco RD, Domeizel M, Guiliano M, Doumenq P, Th F, Théraulaz F (2011) Effects of forest fires on water extractable organic matter and humic substances from Mediterranean soils: UV-vis and fluorescence spectroscopy approaches. *Geoderma* 160:434–443
 43. Jie C, Baohua G, Eugene JL, Hongjun P, Sheng D (2002) Spectroscopic characterization of the structural and functional properties of natural organic matter fractions. *Chemosphere* 48(1):59–68
 44. Iwai H, Fukushima M, Yamamoto M, Komai T, Kawabe Y (2013) Characterization of seawater extractable organic matter from bark compost by TMAH-py-GC/MS. *J Anal Appl Pyrol* 99(3):9–15
 45. Wang Y, Fei Y, Amos B, Gideon O, Moshe H (2010) Extracellular polymeric substances (EPS) in a hybrid growth membrane bioreactor (HG-MBR): viscoelastic and adherence characteristics. *Environ Sci Technol* 44(22):8636–8643
 46. Sheng GP, Yu HQ (2006) Characterization of extracellular polymeric substances of aerobic and anaerobic sludge using three-dimensional excitation and emission matrix fluorescence spectroscopy. *Water Res* 40(6):1233–1239
 47. Tartakovsky B, Sheintuch M, Hilmer JM, Scheper T (2008) Application of scanning fluorometry for monitoring of a fermentation process. *Biotechnol Prog* 12(1):126–131
 48. Wen C, Paul W, Leenheer JA, Karl B (2003) Fluorescence excitation-emission matrix regional integration to quantify spectra for dissolved organic matter. *Environ Sci Technol* 37(24):5701–5710
 49. Coble PG (1996) Characterization of marine and terrestrial DOM in seawater using excitation-emission matrix spectroscopy. *Mar Chem* 51(4):325–346
 50. Liu T, Chen ZL, Yu WZ, You SJ (2011) Characterization of organic membrane foulants in a submerged membrane bioreactor with pre-ozonation using three-dimensional excitation-emission matrix fluorescence spectroscopy. *Water Res* 45(5):2111–2121
 51. Wang Z, Wu Z, Tang S (2009) Characterization of dissolved organic matter in a submerged membrane bioreactor by using three-dimensional excitation and emission matrix fluorescence spectroscopy. *Water Res* 43(6):1533–1540